# Au Nanoparticle Templated Synthesis of pNIPAm Nanogels

Neetu Singh and L. Andrew Lyon*

*School of Chemistry and Biochemistry & Petit Institute for Bioengineering and Bioscience, Georgia Institute of Technology, Atlanta, Georgia 30332-0400*

*Received August 9, 2006. Revised Manuscript Received December 9, 2006*

We have explored a synthetic route toward poly(*N*-isopropylacrylamide) (pNIPAm) nanogels by growing a pNIPAm shell onto a metal nanoparticle seed. Nuclei compatible with precipitation polymerization of thermoresponsive polymers were formed by adsorption of $NH_2$-terminated pNIPAm on Au nanoparticles. The adsorbed pNIPAm layer, when heated above the LCST, collapses onto the Au nanoparticle surface. This polymer layer thus serves as a hydrophobic nucleus for growing pNIPAm oligoradicals during polymer synthesis, resulting in the formation of a pNIPAm shell. Etching of the Au core from the polymer-coated particles with KCN results in hollow hydrogel nanoparticles. The rate of Au core etching as studied by the decrease in Au nanoparticle plasmon absorbance was shown to depend on polymer shell composition, shell thickness, and the thermosensitivity of the polymer. Efficient quenching of fluorophores incorporated in the polymer shell by the core Au nanoparticles was observed; however, the shell fluorescence was regained after core dissolution. Future studies are aimed at understanding the encapsulation of small molecules and proteins within the nanocapsule structure.

## Introduction

The synthesis and application of small hollow polymeric nanoparticles for drug delivery and protein/enzyme encapsulation is an expanding area of research.[1−4] For applications in this area, good control over size on the nanometer scale and low size dispersity is highly desirable. Also required is the ease of conjugation of these nanoparticles to biological macromolecules and their assembly into higher order structures. With advances in the synthesis of polymeric nanoparticles, researchers have designed various interesting architectures, one being the core/shell structure which can provide a robust platform for incorporating multiple orthogonal functionalities into a nanoparticle.[5]

An interesting subclass of polymeric nanoparticles is responsive hydrogel nanoparticles (or nanogels), which are useful in a wide range of applications on account of their stimuli-sensitive phase transition behavior. One of the most commonly studied thermoresponsive polymers is poly(*N*-isopropylacrylamide) (pNIPAm), which undergoes a phase transition from a hydrophilic, water-swollen state to a hydrophobic, globular state when heated to above its lower critical solution temperature (LCST) which is about 31 °C in water. Incorporation of other comonomers can produce a wide variety of stimuli responsivities such as pH, ionic strength, and light. Our group and many others have extensively studied the synthesis, characterization, and applications of such stimuli-responsive materials.[6−8]

In the past, methods toward the production of sub-50 nm polymer particles have utilized cross-linking of block copolymer micelles, metathesis polymerization of covalently bound monomer monolayers, surface-initiated polymerization of monomers in solution, and layer-by-layer adsorption of polyelectrolytes on spherical nanoparticles using a metal-templating method.[9−21] Metal templating is a widely used approach to synthesize hollow nanoparticles. Here, a metal template of desired size can be used to grow a polymer shell, which can be followed by metal dissolution to yield stable hollow polymeric nanoparticles. In this procedure, the size of the inner cavity is basically the diameter of the metal nanoparticles used as the template. Recently, Lee and coworker synthesized hydrogel-coated Au nanoparticles using such a metal-templating approach. They used Au nanopar-

* To whom correspondence should be addressed. E-mal: LL62@mail.gatech.edu.

(1) Meier, W. *Chem. Soc. Rev.* **2000**, *29*, 295.
(2) Langer, R. *Science* **1990**, *249*, 1527.
(3) Peppas, N. A.; Langer, R. *Science* **1994**, *263*, 1715.
(4) Marinakos, S. M.; Anderson, M. F.; Ryan, J. A.; Martin, L. D.; Feldheim, D. L. *J. Phys. Chem. B* **2001**, *105*, 8872.
(5) Nayak, S.; Lee, H.; Chmielewski, J.; Lyon, L. A. *J. Am. Chem. Soc.* **2004**, *126*, 10258.
(6) Nayak, S.; Lyon, L. A. *Angew. Chem., Int. Ed. Engl.* **2005**, *44*, 7686.
(7) Pelton, R. *Adv. Colloid. Interface Sci.* **2000**, *85*, 1.
(8) Wang, C.; Flynn, N. T.; Langer, R. *Adv. Mater.* **2004**, *16*, 1074.
(9) Thurmond, K. B., II; Kowalewski, T.; Wooley, K. L. *J. Am. Chem. Soc.* **1997**, *119*, 6656.
(10) MacKnight, W. J.; Ponomarenko, E. A.; Tirrell, D. A. *Acc. Chem. Res.* **1998**, *31*, 781.
(11) Caruso, F. *Chem. Eur. J.* **2000**, *6*, 413.
(12) Quaroni, L.; Chumanov, G. *J. Am. Chem. Soc.* **1999**, *121*, 10642.
(13) Watson, K. J.; Zhu, J.; Nguyen, S. T.; Mirkin, C. A. *J. Am. Chem. Soc.* **1999**, *121*, 462.
(14) Wu, M.; O'Neill, S. A.; Brousseau, L. C.; McConnell, W. P.; Shultz, D. A.; Linderman, R. J.; Feldheim, D. L. *Chem. Commun.* **2000**, 775.
(15) Huang, H.; Remsen, E. E.; Kowalewski, T.; Wooley, K. L. *J. Am. Chem. Soc.* **1999**, *121*, 3805.
(16) Gittins, D. I.; Caruso, F. *Adv. Mater.* **2000**, *12*, 1947.
(17) Nardin, C.; Thoeni, S.; Widmer, J.; Winterhalter, M.; Meier, W. *Chem. Commun.* **2000**, 1433.
(18) Schneider, G.; Decher, G. *Nano Lett.* **2004**, *4*, 1833.
(19) Marinakos, S. M.; Novak, J. P.; Brousseau, L. C., III; House, A. B.; Edeki, E. M.; Feldhaus, J. C.; Feldheim, D. L. *J. Am. Chem. Soc.* **1999**, *121*, 8518.
(20) Nuss, S.; Bottcher, H.; Wurm, H.; Hallensleben, M. L. *Angew. Chem., Int. Ed. Engl.* **2001**, *40*, 4016.
(21) Li, D.; Jones, G. L.; Dunlap, J. R.; Hua, F.; Zhao, B. *Langmuir* **2006**, *22*, 3344.

10.1021/cm061878d CCC: $37.00 
Published on Web 01/20/2007

**Scheme 1. Au Nanoparticle Templated Synthesis of pNIPAm Nanogels via Aqueous Free-Radical Precipitation Polymerization**

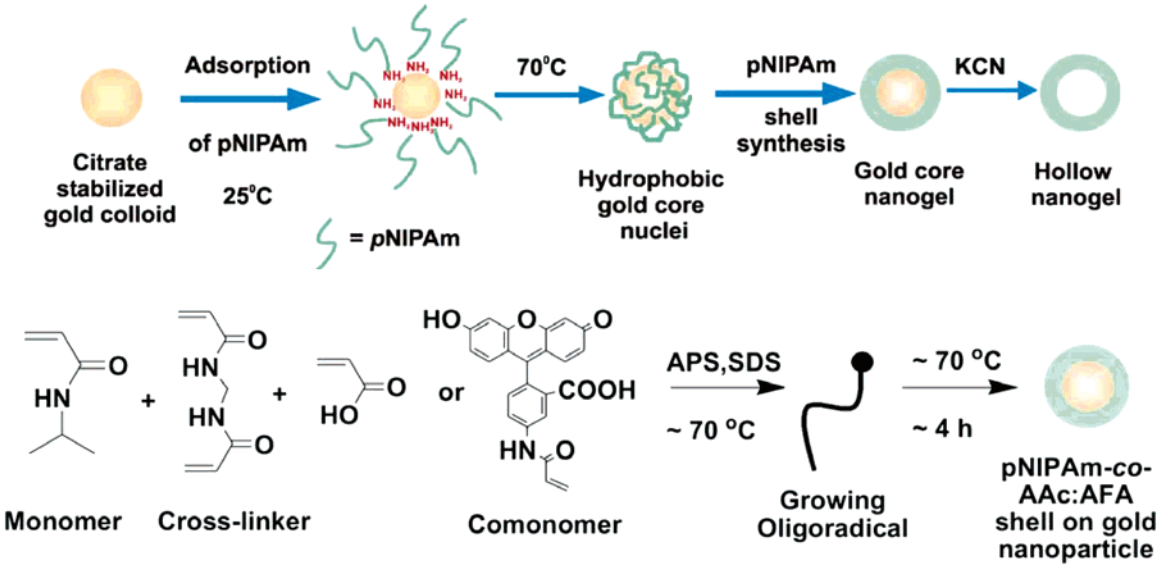


ticles, 60 nm in diameter, as the template and grew a pNIPAm shell by surfactant-free emulsion polymerization.[22] In another example, Fu and co-workers synthesized pNIPAm microcontainers using silica nanoparticle templates.[23] These methods, however, yielded large nanoparticles with radii in the range of 100−200 nm; this size range is typically regarded as not appropriate for many applications in targeted gene and drug delivery. Thus, there still exists a need to develop an in situ free-radical polymerization method for yielding colloidally stable hollow nanogels with good synthetic control over the properties and dimensions in the nanometer range.

In this report, we describe a strategy for synthesizing hollow nanogels based on the widely used sacrificial metal nanoparticle templating method. We have combined the metal-templating approach with a "seed and feed" method previously used by our group to synthesize hydrogel nanoparticles.[24] The seed and feed method involves the initial formation of hydrophobic polymer nuclei, which act as seeds for the precipitation of the growing polymer (feed) chains. When the polymerization conditions are maintained above the polymer's LCST, the growing polymer chains phase-separate and collapse onto the hydrobhobic nuclei to form a cross-linked polymer shell around the core nanoparticle. To make hydrogels with sizes in the range of sub-50 nm, it was envisioned that the use of a small metal nanoparticle-based hydrophobic nucleus can facilitate the formation of a polymer shell with nanometer dimensions. The synthetic route toward the formation of small hollow pNIPAm nanogels involves the in situ polymerization of NIPAm onto Au nanoparticles followed by the dissolution of the Au core as depicted in Scheme 1. This approach can be generalized to synthesize nanogels with the varied sizes and compositions needed for a variety of applications ranging from sensors to cellular biology to delivery vehicles.

## Experimental Section

**Materials.** All materials were obtained from Sigma Aldrich unless otherwise specified. The monomer NIPAm was recrystallized from hexane obtained from J.T. Baker before use. All other chemicals were used as received. Amino-terminated pNIPAm with $M_n$ of 10400 was obtained from Polymer Source Inc. Acetate buffer solution (pH 5.4, 10 mM) was prepared from acetic acid and NaCl obtained from Fischer. Water was distilled and then purified using a Barnstead E-Pure system to a resistance of 18 MΩ and finally filtered through a 0.2 $\mu$m membrane filter (Pall Gelman Metricel) before use.

**Au Nanoparticle Synthesis.** Au colloids were prepared according to a procedure developed by Natan and co-workers.[25] All glassware were cleaned in aqua regia (3 parts HCl, 1 part $HNO_3$) [Caution! aqua regia is corrosive in nature and should be handled with care] and rinsed with deionized water (DI water) before use. First, 500 mL of 0.01% $HAuCl_4$ was brought to boil with vigorous stirring in a round-bottom flask equipped with a condenser. To this solution, 7.5 mL of 1% sodium citrate was added and an instant color change from blue to red-violet was observed. After boiling for 10 min the solution was cooled while stirring for an additional 15 min. Note that transmission electron microscopy (TEM) images of the synthesized colloid showed particles with a mean diameter of 12 nm, while a larger size (mean hydrodynamic radius of 12 nm at 25 °C) was obtained by photon correlation spectroscopy (PCS) measurements.

**Nanogel Synthesis.** To form hydrophobic Au nuclei, the Au colloid was incubated with $NH_2$-terminated pNIPAm. To determine the amount of $NH_2$-terminated pNIPAm required to cover the surface of the Au nanoparticles, the following assay was performed: 500 $\mu$L of 1 M NaCl solution was added to 500 $\mu$L of Au colloid solution after the Au colloid had been incubated overnight with different volumes of 0.1 mM $NH_2$-terminated pNIPAm. The solutions were then kept on a shaker table for 10 min at room temperature. The Au nanoparticle aggregation was monitored by UV−vis spectroscopy by observing the position and shape of the plasmon absorbance peak (vide infra). For the synthesis of the Au core nuclei, Au nanoparticles were mixed on a shaker table with an appropriate amount of $NH_2$-terminated pNIPAm, as determined

(22) Kim, J.-H.; Lee, T. R. *Chem. Mater.* **2004**, *16*, 3647.
(23) Zha, L.; Zhang, Y.; Yang, W.; Fu, S. *Adv. Mater.* **2002**, *14*, 1090.
(24) Jones, C. D.; Lyon, L. A. *Macromolecules* **2000**, *33*, 8301.
(25) Grabar, K. C.; Freeman, R. G.; Hommer, M. B.; Natan, M. J. *Anal. Chem.* **1995**, *67*, 735.

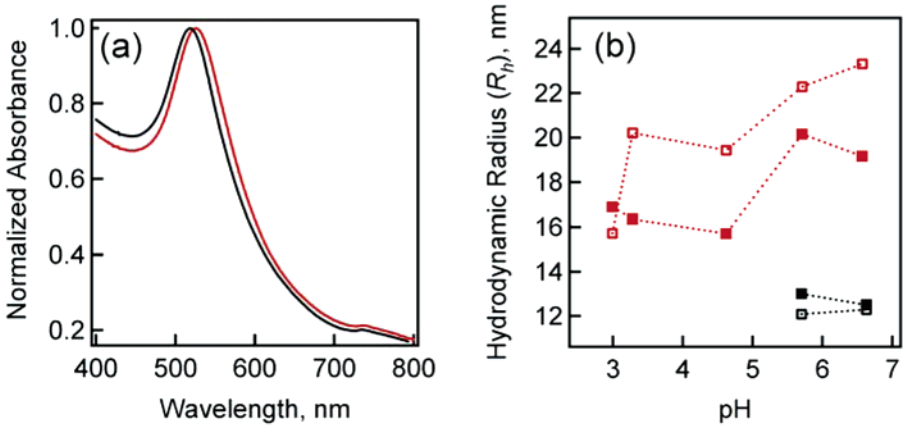


**Figure 1.** (a) Absorption spectra of the Au nanoparticles before (black) and after pNIPAm-*co*-AAc shell synthesis (red). (b) Plot of hydrodynamic radius versus pH at 25 °C (open squares) and 45 °C (filled squares) for Au nanoparticles before (black) and after pNIPAm-*co*-AAc shell synthesis (red).

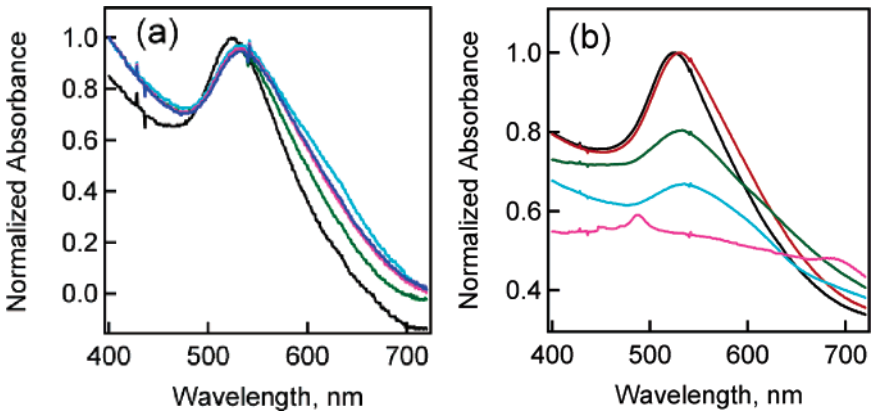


**Figure 2.** Change in absorption spectra following addition of 1,6-hexanedithiol for (a) Au core nanogels and (b) bare Au nanoparticles. Spectra were obtained over time: initial spectrum (black), $t = 0$ min (red), $t = 5$ min (green), $t = 15$ min (cyan), $t = 30$ min (magenta), and $t = 1$ h (blue).

by the aggregation assay, and allowed to incubate with shaking overnight. The solution was cleaned by centrifugation to remove any nonadsorbed $NH_2$-terminated pNIPAm followed by resuspension in DI water. The polymer-adsorbed Au nanoparticles were then heated to ~70 °C under a $N_2$ atmosphere and stirred in a glass vial precleaned with aqua regia. A filtered (using a 0.2 $\mu$m membrane filter) aqueous solution of an appropriate amount of monomer NIPAm, cross-linker *N*,*N*-methylenebis(acrylamide) (BIS), and 65 $\mu$L of 0.1 M aqueous solution of surfactant, sodium dodecyl sulfate (SDS), was added to the reaction vial. After 1 h, the reaction was initiated by injection of 130 $\mu$L of 0.1 M ammonium persulfate (APS) solution and the reaction (total volume = 10 mL) was kept at 70 °C for 4 h. The comonomers acrylic acid (AAc) or 4-acrylamido-fluorescein (AFA) were added just before the reaction initiation to synthesize pNIPAm-*co*-AAc or fluorescent pNIPAm-*co*-AFA nanogels. A molar composition of 85% monomer, 5% cross-linker, and 10% comonomer was used. The total monomer concentration used in the shell synthesis was 0.25, 0.5, or 1.0 mM. The synthesized Au core nanogels were cleaned by several cycles of centrifugation/resuspension.

**Dissolution of the Au Core.** Following shell synthesis, the template Au cores were dissolved by adding 0.1 M KCN solution to a clean Au core nanogel solution while stirring. The core dissolution was monitored by the disappearance of the Au plasmon absorption band using UV−vis spectroscopy. For studying the etching rate, 1 mL of the Au core nanogel solution was etched using 0.5 mL of a 0.1 M KCN solution. Etching was also studied at a higher temperature by monitoring the etching of the nanogel solution (equilibrated for 30 min at 45 °C) after addition of the KCN solution which was also maintained at 45 °C. The hollow nanogels were then purified by dialysis using Spectra/Por 10000 MWCO dialysis membrane (VWR) against DI water for ~2 weeks with the water being changed twice per day.

**UV−Vis Spectroscopy.** All absorption spectra were obtained in quartz cuvettes using a Shimadzu UV 1601 spectrophotometer equipped with a recirculating water bath based temperature controller.

**Photon Correlation Spectroscopy.** Particle sizes were determined by photon correlation spectroscopy (PCS, Protein Solution Inc.) equipped with an integrated Peltier temperature control device which gives temperature accuracy within ±0.1 °C. The instrument collects scattered light at 90° with a single-mode optical fiber coupled to an avalanche photodiode detector. The samples were thermally equilibrated at each temperature for 10 min before measurement. The data presented is an average of at least 15 measurements with acquisition time of 10 s. The hydrodynamic radii of the particles were calculated from the diffusion coefficients using the Stokes−Einstein equation. All the data analysis was done using Dynamic Software version 5.25.44 provided by Protein Solutions Inc.

**Transmission Electron Microscopy.** The synthesized nanoparticles were imaged on a JEOL 100CX II (100 kV) transmission electron microscope (TEM). All TEM samples were prepared by casting a drop of the nanoparticle solution (diluted 10 times) on a Formvar-coated Cu TEM grid (Ted Pella) placed on a Kimwipe. The grid was then dried overnight at ambient temperature. For the imaging of the hydrogel nanoparticles following core etching, the AAc groups in the polymer shell were stained with an electron microscopy contrast agent. Briefly, 0.050 mL of 1 mM pNIPAm-*co*-AAc nanogels following dissolution of the gold cores and dialysis was mixed with 0.5 mL of 1 mM uranyl acetate (Polysciences) and stirred for 1 h.

**Table 1. Hydrodynamic Radii ($R_h$) Determined by PCS**

| | pNIPAm nanogels[a] (in DI water) | | pNIPAm-*co*-A ac nanogels[a] (in pH 5.4 buffer solution) | |
|---|---|---|---|---|
| total monomer concentration (mM) | average[b] $R_h$ at 25 °C (nm) | average[b] $R_h$ at 45 °C (nm) | average[b] $R_h$ at 25 °C (nm) | average[b] $R_h$ at 45 °C (nm) |
| 0.25 | 15 ± 1 | 13 ± 1 | 19 ± 2 | 18 ± 1 |
| 0.50 | 23 ± 2 | 16 ± 0.3 | 27 ± 2 | 19 ± 0.2 |
| 1.00 | 30 ± 1 | 19 ± 0.4 | 39 ± 3 | 27 ± 1 |

[a] The nanogels contain a Au core with $R_h$ of 12 ± 0.6 nm at 25 °C and 13 ± 0.3 nm at 45 °C. [b] Average of three measurements.

**Atomic Force Microscopy.** All the images were obtained in ac mode on an Asylum Research MFP-3D atomic force microscope (AFM). Spring constants were calculated using the thermal method. Imaging and analysis was performed using the Asylum Research MFP-3D software (IgorPro, WaveMetrics, Inc., Lake Oswego, OR). An Olympus AC160 cantilever with $k = 42$ N/m, $f_0 = 300$ kHz was used for imaging. AFM samples were prepared by casting a drop of the sample on micro cover glass slips (VWR) and drying overnight. Images were also obtained on cationic glass cover slips. Briefly, glass cover slips were first treated in an Ar plasma (Harrick Scientific) for 30 min followed by immersion of the glass substrate in 1% 3-aminopropyltrimethoxysilane solution in absolute ethanol (200 proof) for ~2 h. They were rinsed several times with 95% ethanol followed by rinsing with DI water and drying in a stream of $N_2$ gas. One drop of 1 mM pNIPAm-*co*-AAc nanoparticle solution was cast onto the functionalized glass substrate. After 15 min, the substrate was immersed in DI water for 2 h, rinsed with DI water, and dried with $N_2$ gas, leaving behind nanoparticles that are strongly attached to the cationic substrate by Coulombic interactions.

**Dithiol Aggregation Studies.** To prepare samples for dithiol-induced aggregation, 0.5 mL of the bare Au colloid and the clean Au core nanogels were centrifuged and redispersed in 0.5 mL of ethanol. A 0.1 mL sample of 1,6-hexanedithiol dissolved in 0.4 mL of ethanol was added to the solutions, which were then agitated on a shaker table. The solutions were monitored by UV−vis spectroscopy to observe the changes in the Au plasmon band at various time intervals.

**Fluorescence Spectroscopy.** All emission measurements were done using a Photon Technology International fluorescence spectrophotometer, equipped with a Model 814 PMT photon-counting detector. The slits were adjusted to achieve a spectral bandwidth of 2 nm and the spectra were obtained with a 1 nm step size and a 1 s integration time. The samples were excited at a wavelength of 478 nm.

## Results and Discussion

Citrate-stabilized Au nanoparticles synthesized by the reduction of $HAuCl_4$ were used for the formation of polymerization seeds due to the ease of their preparation and characterization. The UV−vis spectra for the synthesized colloid showed an absorption band with a maximum around 518 nm due to the well-known surface plasmon resonance of spherical Au nanoparticles.[26] Seeds compatible with the precipitation polymerization of NIPAm were formed by the adsorption of a layer of amino-terminated pNIPAm onto the Au nanoparticles.[27,28] When heated to 70 °C (above the LCST of pNIPAm), the adsorbed pNIPAm layer collapses onto the

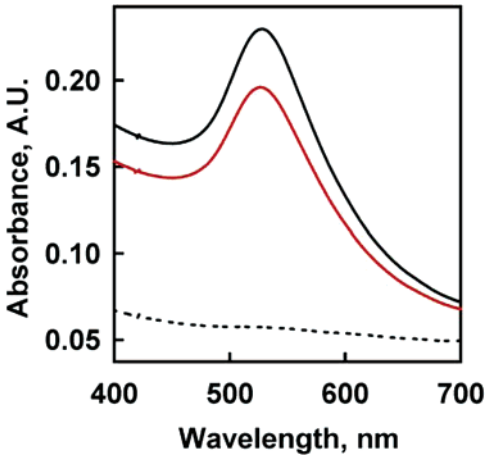


**Figure 3.** Decrease in Au plasmon absorbance after addition of KCN to Au core pNIPAm nanoparticles synthesized using a 0.5 mM total monomer concentration. The spectrum shown in black was obtained before KCN addition, whereas the spectrum shown in red was taken immediately (<20 s) after addition. The spectrum shown as a black dashed line was obtained after 1 day.

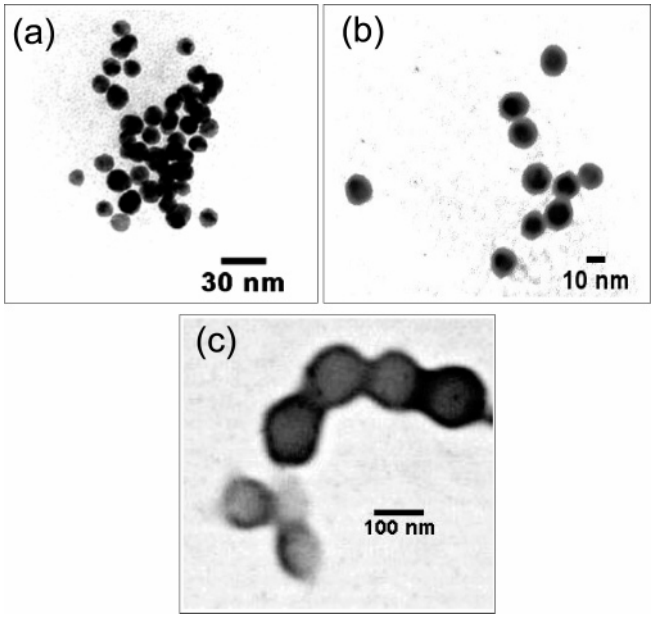


**Figure 4.** TEM image of (a) bare gold nanoparticles, (b) 1 mM pNIPAm-*co*-AAc nanogels containing gold nanoparticle template cores, and (c) 1 mM pNIPAm-*co*-AAc nanogels after core etching and uranyl acetate staining.

Au nanoparticle surface, thus serving as a hydrophobic nucleus for the subsequent precipitation polymerization step. To avoid the formation of separate hydrophobic nuclei from any excess pNIPAm in solution (not adsorbed on Au), we determined the minimum amount of polymer required for surface coverage of the Au nanoparticles. It is well-known that citrate-stabilized Au nanoparticles tend to aggregate on the addition of NaCl, resulting in the red shift of the nanoparticle absorption band, whereas protein or polymer-protected Au nanoparticles resist salt-induced aggregation. The minimum amount of $NH_2$-terminated pNIPAm required for complete surface coverage of the Au nanoparticles was determined by monitoring the resistance of the Au colloid

(26) Link, S.; El-Sayed, M. A. *J. Phys. Chem. B* **1999**, *103*, 4212.
(27) Plunkett, M. A.; Wang, Z.; Rutland, M. W.; Johannsmann, D. *Langmuir* **2003**, *19*, 6837.
(28) Seker, F.; Malenfant, P. R. L.; Larsen, M.; Alizadeh, A.; Conway, K.; Kulkarni, A. M.; Goddard, G.; Garaas, R. *Adv. Mater.* **2005**, *17*, 1941.

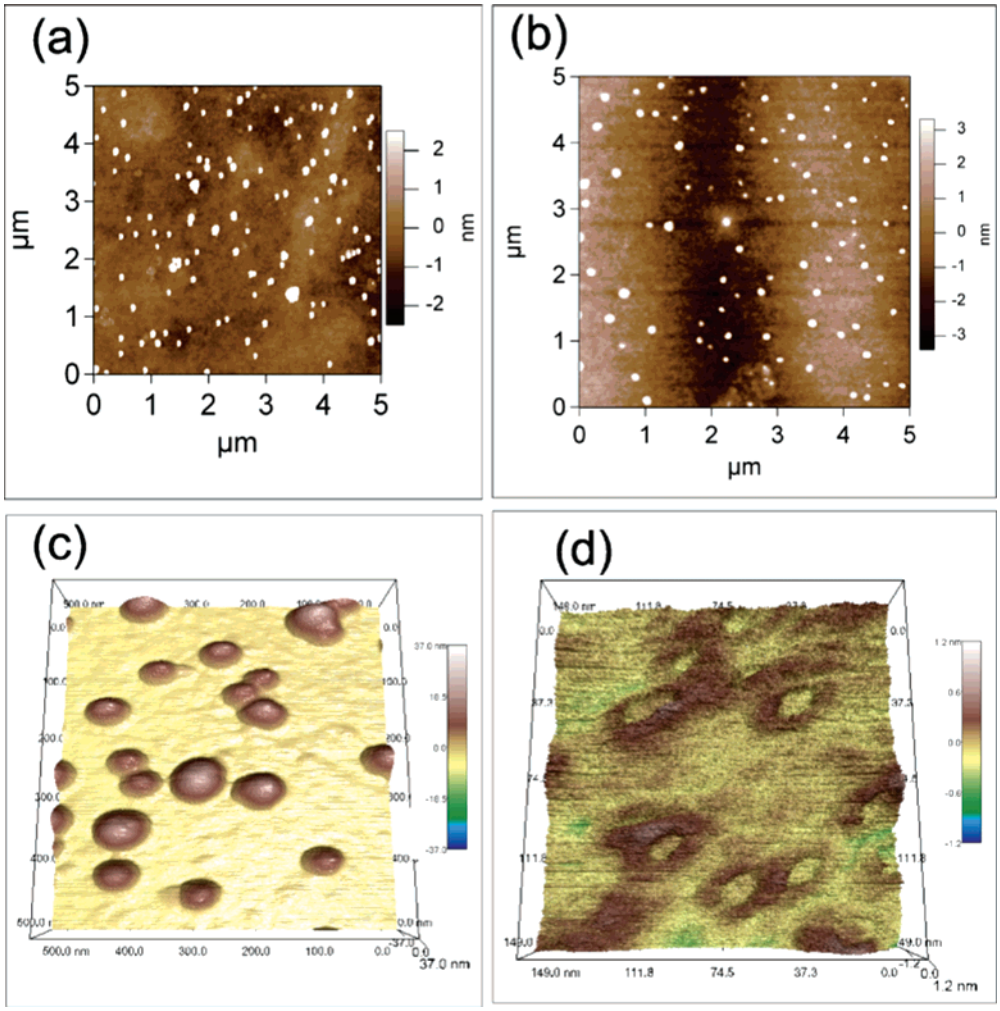


**Figure 5.** AFM images of 1 mM pNIPAm-*co*-AAc nanogels on a glass substrate, (a) before and (b) after etching of the gold template cores. 3D rendering of AFM images of 1 mM pNIPAm-*co*-AAc nanogels on aminosilane-functionalized glass substrate, (c) before and (d) after etching of the gold cores.

toward NaCl-induced aggregation by following the red shift in the plasmon absorption band. Onto these polymer-stabilized Au nanoparticles, pNIPAm shells were synthesized by free-radical polymerizaton as described in the Experimental Section. To form pH-responsive nanogel particles, acrylic acid (AAc) was used as the comonomer. It should be noted that the amount of monomer used for the synthesis was also kept at very low concentrations to avoid the formation of separate (non-Au-containing) nuclei in the reaction solution.

Due to the presence of Au cores, it is easy to characterize the synthesized nanogels by UV−vis spectroscopy. The absorption spectra of the Au nanoparticles before and after shell synthesis are shown in Figure 1a. The plasmon band for the Au-core nanogels has a maximum ($\lambda_{max}$) around 526 nm. There was no evidence of aggregation of the Au colloid after the polymer shell synthesis. The plasmon absorption band reflects an isolated Au nanoparticle core encapsulated by a polymer shell rather than multiple Au particles trapped in close proximity within the polymer gel. A slight red shift in the plasmon band is observed due to an increase in the refractive index around the Au nanoparticle due to the polymer shell ($RI_{polymer} > RI_{water}$).[29]

Particle size (via PCS) measurements of the nanogels revealed a mean hydrodynamic radius ($R_h$) ranging from 20 to 80 nm depending on the monomer concentration used in synthesis. The (pNIPAm-*co*-AAc)-coated Au nanoparticles show a decrease in size at high temperature and low pH (Figure 1b) as a result of the dual (pH and temperature) responsivity of the hydrogel. Note that the uncoated Au nanoparticles (black symbols) aggregated at low pH due to the presence of salt in the buffer solution. However, the nanogels showed no aggregation under any of the studied conditions, suggesting that the Au cores in these particles were well-protected.

The nanogels were also stable to more effective aggregating agents such as 1,6-hexanedithiol. These results further confirm the passivating nature of the cross-linked pNIPAm shell (Figure 2a). The uncoated Au nanoparticles, on addition of 1,6-hexanethiol (Figure 2b), show a greatly red-shifted absorption spectrum with diminished intensity, indicating extensive particle aggregation. On the other hand, the Au-core nanogel solution shows very limited aggregation (Figure 2a). The slight changes in peak breadth observed here may be due to some amount of non-polymer-coated Au nanoparticles remaining in the solution. Interestingly, the aggregation with hexanedithiol could therefore be used as a method for separating non-polymer-coated Au nanoparticles

(29) Underwood, S.; Mulvaney, P. *Langmuir* **1994**, *10*, 3427.

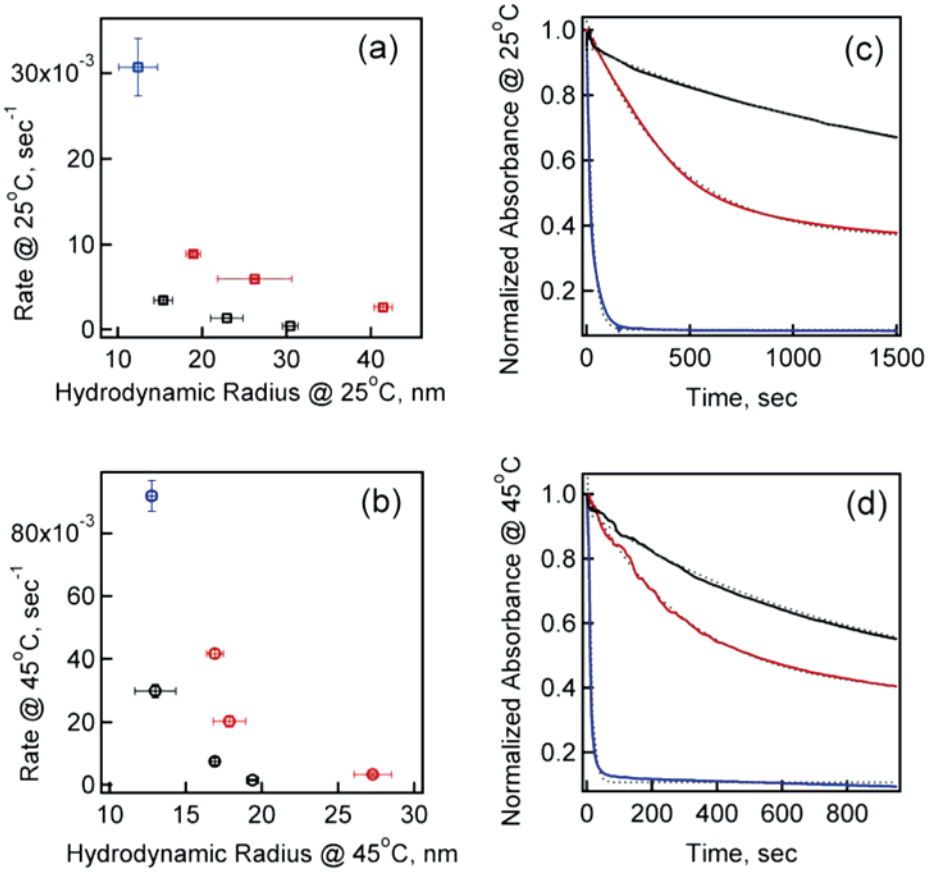


**Figure 6.** Etching rates of Au cores in water at (a) 25 °C and (b) 45 °C for bare Au (blue) and pNIPAm (black) and pNIPAm-*co*-AAc (red) nanogels plotted against the hydrodynamic radius. Absorbance of Au nanoparticles at $\lambda_{max}$ with respect to time at (c) 25 °C and (d) 45 °C for bare Au (blue), 1 mM pNIPAm nanogel (black), and 1 mM pNIPAm-*co*-AAc nanogel. The dotted curves (gray) are the exponential fit to the data. Each data point is an average from three different experiments.

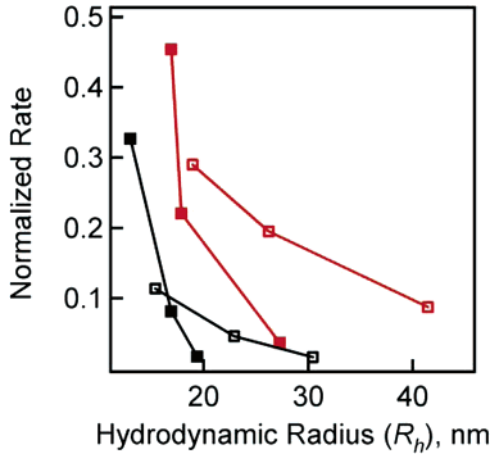


**Figure 7.** Effect of shell thickness and shell deswelling on the etching rate of Au cores from pNIPAm (black) and pNIPAm-*co*-AAc (red) nanogels. The rate of Au core etching for the nanogels were normalized with respect to the rate of bare Au etching at particular temperatures. Open square symbols are rates at 25 °C and filled square symbols are rates at 45 °C.

from the nanogels following synthesis, which is otherwise difficult to accomplish via centrifugation.

Nanogels of pNIPAm and pNIPAm-*co*-AAc with different shell thicknesses (Table 1) were synthesized by varying the total monomer concentration (0.25, 0.5, and 1 mM) while keeping the cross-linker (5 mol %) and comonomer (10 mol % AAc) percentage, surfactant, and initiator concentrations the same across all batches. Nanogels with AAc comonomer in the polymer shell were larger in size ($R_h$) as compared to nanoparticles without AAc at the same total monomer concentration. This size difference could be due to the repulsive interaction between the charged carboxyl groups in the AAc shell or the greater free energy of mixing with water due to the more hydrophilic nature of the pNIPAm-*co*-AAc polymer.

To obtain hollow nanogels from the Au core nanogels, the Au was dissolved by the addition of a 0.1 M KCN solution. Gold etching occurs via transport of the etchant (cyanide ion) through the polymer shell to the core, where $Au^0$ is converted to $[Au(CN)_4]^-$ in the presence of oxygen.[30,31] The Au core etching was followed by a loss of the Au plasmon absorbance. An example of core etching for Au core pNIPAm nanoparticles synthesized using a 0.5 mM total monomer concentration has been shown in Figure 3.

To characterize the architecture, shape, and morphology of the nanogels before and after dissolution of the templating core, TEM and AFM imaging was performed. Figure 4 shows representative TEM images of 1 mM pNIPAm-*co*-AAc nanogels before (Figure 4b) and after dissolution (Figure 4c) of the templating gold cores (Figure 4a). Nanogels following gold core dissolution were imaged by the staining of the AAc groups in the polymer shell with uranyl acetate. As seen from Figure 4c, the polymer shell

(30) Paulini, R.; Frankamp, B. L.; Rotello, V. M. *Langmuir* **2002**, *18*, 2368.
(31) Templeton, A. C.; Hostetler, M. J.; Kraft, C. T.; Murray, R. W. *J. Am. Chem. Soc.* **1998**, *120*, 1906.

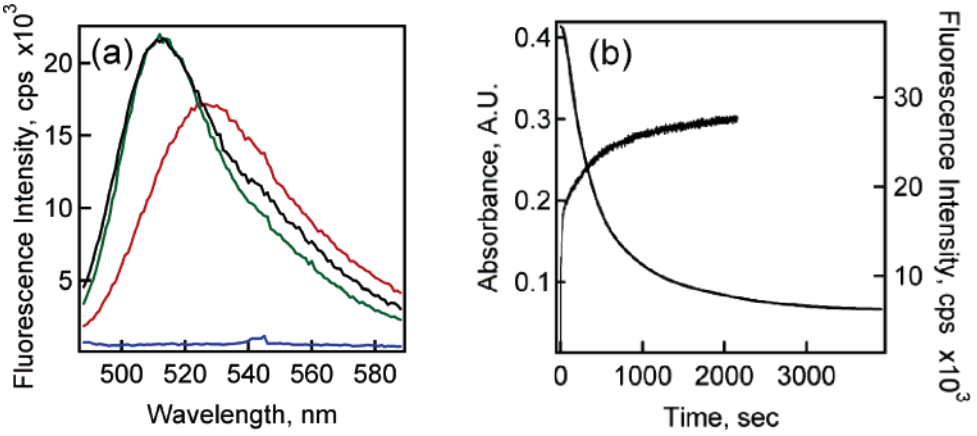


**Figure 8.** (a) Fluorescence quenching of shell fluorophores due to the close proximity of Au nanoparticles. Fluorescence spectrum of pNIPAm-*co*-AFA particles before (blue) and after (red) Au core dissolution. No fluorescence quenching was observed in a physical mixture of AFA and bare Au (green) when compared to AFA solution (black). (b) Disappearance of absorbance intensity (525 nm) of Au nanoparticle and appearance of fluorescence intensity of the shell fluorophore (525 nm) with respect to time follows the progress of core dissolution. $\lambda_{exc}$= 478 nm.

integrity is maintained following the dissolution of the gold cores. Note that soft hydrogel nanoparticles following core dissolution tend to flatten on the TEM grid during sample preparation and imaging conditions. Thus, size determination of the hollow nanogels cannot be reliably done based on these images.

Figure 5 shows AFM images of 1 mM pNIPAm-*co*-AAc nanogels. AFM images of particles deposited on a glass substrate show feature heights in the range of 10−15 nm (see Supporting Information) before the dissolution of the templating cores (Figure 5a), which correlates well with the diameter of the gold core inside the nanogels. A similar height range was observed for images obtained on a functionalized glass substrate in which case the polymer shell has strong interactions with the substrate. However, the soft nature of the nanogels following core dissolution is clearly reflected in Figures 5b and 5d. Images obtained on a simple glass substrate showed heights in the range of 6−10 nm (Figure 5b) whereas when imaged on functionalized glass substrate (Figure 5d), the nanoparticles appear to be flattened on the substrate due to strong polymer−substrate interactions. The hollow nature of the nanogels is clearly observable in Figure 5d. AFM imaging thus also gives a strong indication of the variation in the nanoparticle sizes due to the particle−substrate interactions, as was observed in the TEM analyses.

The effect of polymer shell thickness and composition on the Au core etching rate was investigated. Figure 6a shows the etching rates of Au cores of pNIPAm and pNIPAm-*co*-AAc nanogels for different polymer shell thicknesses at 25 °C. The etching rates were obtained by fitting the plot of the observed decrease in absorbance with time as shown in Figures 6c and 6d. The slower etching rates for the polymer-coated Au nanoparticles relative to uncoated ones indicate that the polymer shell indeed slows down the etching process. Furthermore, the etching rate decreased with increasing polymer thickness ($R_h$) for both types of nanogels. Interestingly, pNIPAm-*co*-AAc nanogels showed a faster Au etching rate as compared to pNIPAm nanogels synthesized with the same monomer concentration. The AAc carboxyl groups and the larger free volume of pNIPAm-*co*-AAc may facilitate the diffusion of cyanide ions through the polymer shell relative to pNIPAm shells. The effect of polymer deswelling on the etching rate was also studied by following the etching at 45 °C, a temperature above the LCST of the nanogels (Figure 6b). The measured etching rate for the polymer-coated nanoparticles was normalized to that of the uncoated Au nanoparticles to account for any intrinsic temperature dependence of the etching chemistry (Figure 7). The temperature-induced deswelling of the polymer shell significantly increases the etching rate for 0.25 and 0.5 mM pNIPAm and pNIPAm-*co*-AAc nanogels, but for 1 mM nanogels the change was insignificant as evident from Figure 7. Apparently, for thinner coatings the major factor controlling the etching rate is the absolute thickness of the hydrogel coating, regardless of its degree of solvation (above vs below the LCST). However, one should note the presence of other complicating factors such as the decrease in the ionic diffusion resulting from the reduced porosity of the deswollen polymer shell. This factor may become more important as the shell thickness increases. The details of ionic transport through these shells therefore deserve further investigation; we are currently performing such studies in our group.

To facilitate particle characterization, we incorporated a fluorescent comonomer, 4-acrylamido-fluorescein (AFA), into the polymer shell during polymerization. Gold nanoparticles are known to quench the emission of fluorophores in close proximity via efficient resonance energy transfer.[32,33] We observed that indeed the fluorescence from the shell-incorporated AFA was quenched (Figure 8a), thus giving additional confirmation that our synthesis yielded a Au core surrounded by a thin pNIPAm-*co*-AFA shell. A control study with the Au colloid incubated with a solution of AFA showed no loss in the fluorescence intensity. In fact, the AFA fluorescence in the nanogels was regained when the Au core was etched, resulting in fluorescent, hollow nanogel particles. Figure 8a shows the increase in the

(32) Fan, C.; Wang, S.; Hong, J. W.; Bazan, G. C.; Plaxco, K. W.; Heeger, A. J. *Proc. Natl. Acad. Sci. U. S. A.* **2003**, *100*, 6297.
(33) Dulkeith, E.; Morteani, A. C.; Niedereichholz, T.; Klar, T. A.; Feldmann, J.; Levi, S. A.; van Veggel, F. C. J. M.; Reinhoudt, D. N.; Moller, M.; Gittins, D. I. *Phys. Rev. Lett.* **2002**, *89*, 203002.

fluorescence of the pNIPAm-*co*-AFA nanogel solution following cyanide etching of the Au cores. The evolution of the fluorescence intensity follows the progress of the etching process (see Figure 8b) in a manner similar to the observed decrease in plasmon absorbance resulting from the etching of the Au.

## Conclusions

In conclusion, we have developed a synthetic route to synthesize nanosized, hollow pNIPAm hydrogel particles via a straightforward precipitation polymerization method. The sub-50 nm dimensions make the nanogels ideal for drug and gene delivery, for cellular imaging, as nanoreactors, as protective shells for enzymes, and as transfection vectors in gene therapy. The presence of carboxyl functional groups not only gives pH responsivity to the nanoparticles but also gives a handle to tune the properties by providing convenient handles for postpolymerization modification/bioconjugation. Incorporation of the fluorescent monomer not only helps in easy characterization but also adds a useful property to the nanogel for their possible use in sensing and imaging applications. These attributes combined with the ability to tune the particle size as well as the inner cavity makes the nanogels attractive for biological applications. Future studies are aimed at understanding the encapsulation of small molecules and proteins within the hollow nanogels.

**Acknowledgment.** L.A.L. gratefully acknowledges financial support from the National Science Foundation, Division of Materials Research (DMR-0203707). We acknowledge the Center for Nanostructure Characterization and Fabrication at Georgia Tech for the Transmission Electron Microscopy facilities.

**Supporting Information Available:** AFM image feature height profiles of 1 mM pNIPAm-*co*-AAc nanogels before and after gold core etching on glass and aminosilane-functionalized glass. This material is available free of charge via the Internet at http://pubs.acs.org.

CM061878D